Modeling of Brightness Fields of Ice-Crystal Broken Clouds

A. G. Petrushin
Institute of Experimental Meteorology
Obninsk, Russia

T. B. Zhuravleva
Institute of Atmospheric Optics
Tomsk, Russia

Introduction

The real clouds are highly variable in space; therefore, the radiative transfer modeling of fluxes and brightness fields of the atmosphere—an underlying surface system, must account for cloud field structure on much smaller scales than the resolution of the atmospheric general circulation models. In the last few years, most research effort was directed toward the study of liquid-water clouds, whereas the influence of horizontal inhomogeneity on radiative transfer in ice clouds was of much less concern (Liou and Rao 1996; Fu et al. 2000; Macke et al. 2000). This was mostly due to the difficulty of determining the microstructure of real ice clouds, primarily because ice crystals in the atmosphere have different shapes, wide range of sizes and orientations in the space, etc. Also to calculate the radiative properties of horizontally homogeneous clouds, it is generally sufficient to know the asymmetry parameter, single scattering albedo, and extinction coefficient. Within the framework of current microstructure models, well-developed parameterizations exist, quite efficient and convenient for application (Fu and Liou 1993; Mitchell et al. 1996).

This work is aimed to estimate the influence of cloud field random geometry on brightness fields of ice clouds in the narrow bands of near-infrared (IR) spectral range. The single-scattering properties (scattering phase function, single-scattering albedo, and extinction coefficient) of the ice cloud micro-structure model, with ice particles shaped as the solid hexagonal plates and columns, are calculated by the method of geometric optics taking diffraction into account. The present work continues the earlier effort devoted to the study of combined influence of the random cloud geometry and ice particle shapes and size distribution on radiative properties of ice-crystal clouds (Petrushin and Zhuravleva 2000).

Scattering of Optical Radiation by Ice-Crystal Cloud

Consider an ice cloud composed of ice plates and columns. We assume the mean cloud temperature is about – 40°C, under which conditions the concentration of supercooled cloud particles in the ice cloud can be considered negligibly small compared with a concentration of ice crystals (Sundqvist 1993).

The ice particle size distribution in ice clouds can be represented as:

$$f(l, D, d, h) = f_{col}(D, l) + f_{pl}(d, h)$$

Where f_{col}(D,1) is the size distribution function of ice columns, D and l are the diameter and length of column; f_{pl}(d,h) is the ice plate size distribution function, and d and h are the plate diameter and thickness, respectively. The distribution functions f_{col}(D,1) and f_{pl}(d,h) can be found in Petrushin (1998).

The characteristics of radiation scattered by ice cloud medium (scattering phase function $P(\theta)/4\pi$, scattering, extinction, and absorption coefficients α, ε, and β, and single scattering albedo ω) are related to the corresponding characteristics of each cloud ice phase (fraction) via the coefficients g_{col} and g_{pl} as:

$$P(\theta)/4\pi = g_{pl} \times P_{pl}(\theta)/4\pi + g_{col} \times P_{col}(\theta)/4\pi, \quad 1/\omega = g_{pl}/\omega_{pl} + g_{col}/\omega_{col},$$

$$\alpha = \alpha_{pl} + \alpha_{col}, \ \beta = \beta_{pl} + \beta_{col}, \ \varepsilon = \varepsilon_{pl} + \varepsilon_{col},$$

where $g_{col} = \alpha_{col}/(\alpha_{col} + \alpha_{pl})$, $g_{pl} = 1 - g_{col}$

The characteristics of the scattering optical radiation by ice columns and plates were calculated as described by Petrushin (1998). As initial ice crystal sizes, we took: modal diameter of ice plates $d_{mod} = 40\ \mu m$ and mean length of ice columns $l_0 = 50\ \mu m$; while the ratio of prism- to plate -shaped crystal concentrations for Cirrus clouds was assumed to be $N_{col}/N_{pl} \approx 3$ (Heymsfield and Platt 1984). (Recall that ice crystals of these sizes have chaotic orientation in space [Sundqvist 1993]). The complex refractive indices for ice m_i at different wavelengths λ were taken from Warren (1984).

Calculations of scattering efficiency factors K (Table 1) indicate that, for infrared wavelengths considered here, the mean ratio $K_{pl}/K_{col} \approx 1.02$, which almost coincides with $K_{pl}/K_{col} \approx 1.03$ at λ = 0.63 μm. Therefore, for ice crystal microstructure considered here, we set $g_{col} \approx 0.53$.

Table 1. Calculations of scattering efficiency factors K for four different wavelengths.

λ, μm	$m_i = n - i \times \kappa$	K_{pl}	K_{col}	K_{pl}/K_{col}
0.63	1,31 -i×1,04(-8)	2.09	2.03	1.03
2.60	1.202- i×1.01(-3)	2.07	1.87	1.10
3.08	1.325- i×6.25(-1)	1.21	1.21	1.00
3.97	1.365- i×9.16(-3)	1.52	1.60	0.95

Figure 1 presents results of calculations of scattering phase functions for ice cloud at IR wavelengths. Except for small (refractive) scattering angles and halo region, the scattering phase function for λ = 0.63 μm practically coincides with those for ice plates and columns, presented earlier (Petrushin 1998; Petrushin and Zhuravleva 2000); so it is not presented here. The comparison of scattering phase

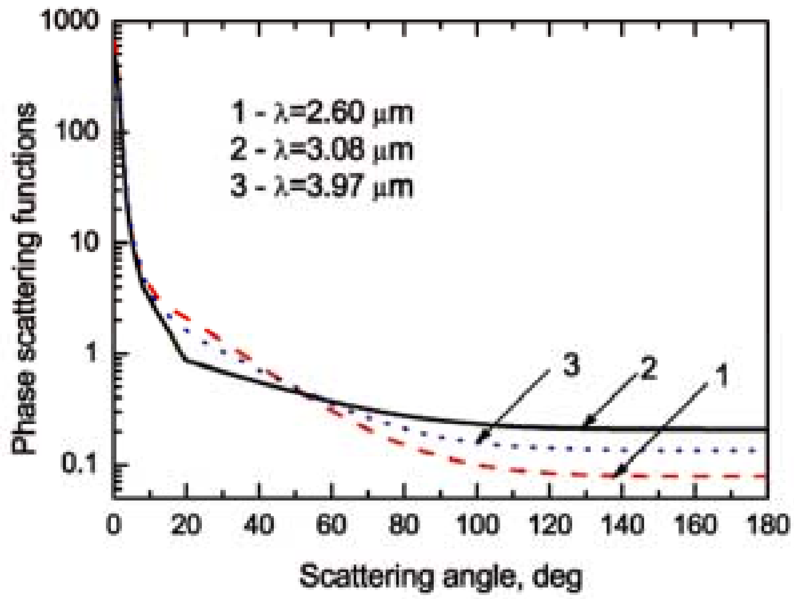

Figure 1. Scattering phase functions for wavelengths λ = 2.6μm, λ = 3.08 μm, and λ = 3.97 μm. Calculations are made for systems of ice plates and columns by the method of Petrushin (1998).

functions for different wavelengths shows that, for large imaginary parts m_i, i.e., in presence of strong absorption of infrared radiation, there is almost no refraction by particles and almost no halo effects of nonspherical (hexagonal) particles. Outside of the halo region, the calculated scattering phase functions qualitatively agree with those calculated for other infrared wavelengths (Cai and Liou 1985) for which $\kappa \sim 10^{-3}$. For $\kappa > 10^{-3}$, the scattering phase function calculated by ourselves for λ = 3.08 μm qualitatively agrees with scattering phase function for λ =10.6 μm (m_i = 1.097- i×1.34 [-1]) over an entire range of scattering angles (Cai and Liou 1985).

Brightness Fields of Ice-Crystal Broken Clouds

The random nature of real broken clouds gives no way to uniquely describe the cloud-radiation interaction; therefore, as before (Petrushin and Zhuravleva 2000), we will use the statistical description of radiative transfer in clouds.

Model and Method. We will characterize the mean angular distributions of upward (↑) and downward (↓) solar radiances in terms of the quantity

$$\tilde{I}^{\uparrow(\downarrow)}(z_*, \mu_i, \mu_{i+1}) = \frac{1}{2\pi(\mu_{i+1} - \mu_i)} \times \int_{\mu_i}^{\mu_{i+1}} \int_{2\pi} I^{\uparrow(\downarrow)}(z_*, \mu, \varphi) d\varphi d\mu$$

where $I(z,\mu,\varphi)$ is the mean scattered intensity in direction $\vec{\omega} = (\xi, \varphi), \mu = \cos\xi$, at the level $z = z_*$. The integration limits (μ_i,μ_{i+1}) are chosen such that the difference between the corresponding zenith angles satisfies the relation $|\xi_i - \xi_{i+1}| = 5^\circ$.

Model of the cloudy-aerosol atmosphere and the Monte Carlo algorithm for calculating mean upward and downward fluxes of solar radiation in the near-IR spectral range are given in Titov and Zhuravleva (1997) in detail. It is assumed that a unit flux of solar radiation is incident on the top of the atmosphere H_{atm}^{top} in the direction $\vec{\omega} = (\xi_\oplus, \varphi_\oplus)$, where $\xi_\oplus$ and $\varphi_\oplus$ are zenith and azimuth solar angles. Underlying surface reflects according to Lambert law. We treat the transmission by water vapor and carbon dioxide using transmission function, as described by Moskalenko (1969):

$$P_{\Delta\nu} = \exp\left[-\beta_{\Delta\nu}\left(w^*\right)^{m_{\Delta\nu}}\right]$$

with spectral resolution $\Delta\nu \approx 20\,\mathrm{cm}^{-1}$. Here w^* is the equivalent (reduced) absorber mass, which in layer (z_1, z_2) of plane-stratified atmosphere is given by

$$w^* = \frac{1}{\cos\theta}\int_{z1}^{z2} \rho(z)\left(\frac{p(z)}{p_0}\right)^{n\Delta\nu} dz$$

where $\rho(z)$ and $\rho(z)$ are the absorber density and pressure (in atm) at height z; p_0 = 1atm, and θ is the viewing zenith angle.

Calculation Results. The angular distributions of solar radiation are calculated for three wavelengths: $\lambda = 0.63\mu m$ (no absorption), $\lambda = 3.08\mu m$ (weak absorption by water vapor and strong absorption by ice particles, $\omega = 0.56$), and $\lambda = 3.97\mu m$ ($\omega = 0.69$). It is assumed that $H_{atm}^{top} = 16$ km; clouds occupy the layer 7 to 9 km; solar azimuth angle $\varphi_\oplus = 0$; the vertical profile of water vapor is chosen to correspond to mid-latitude summer. In what follows, we present calculations of $\tilde{I}^{\uparrow(\downarrow)}$ at the levels $z = H_{atm}^{top}$ and z = 0, respectively.

Figure 2 presents angular distributions of upward and downward solar radiances under overcast conditions for $\lambda = 3.08\mu m$, from which we can estimate the sensitivity of $\tilde{I}^{\uparrow(\downarrow)}$ to such factors as scattering phase function (assuming no water vapor and ice particle absorption), ice particle absorption (assuming no water vapor absorption), and water vapor absorption. Because clouds are considered to be located quite high above the surface, the absorption by water vapor will be less significant in above-cloud atmosphere than below the cloud. Therefore, it is expected that the absorption by H_2O will have a larger effect on angular structure of radiation in below-cloud layer.

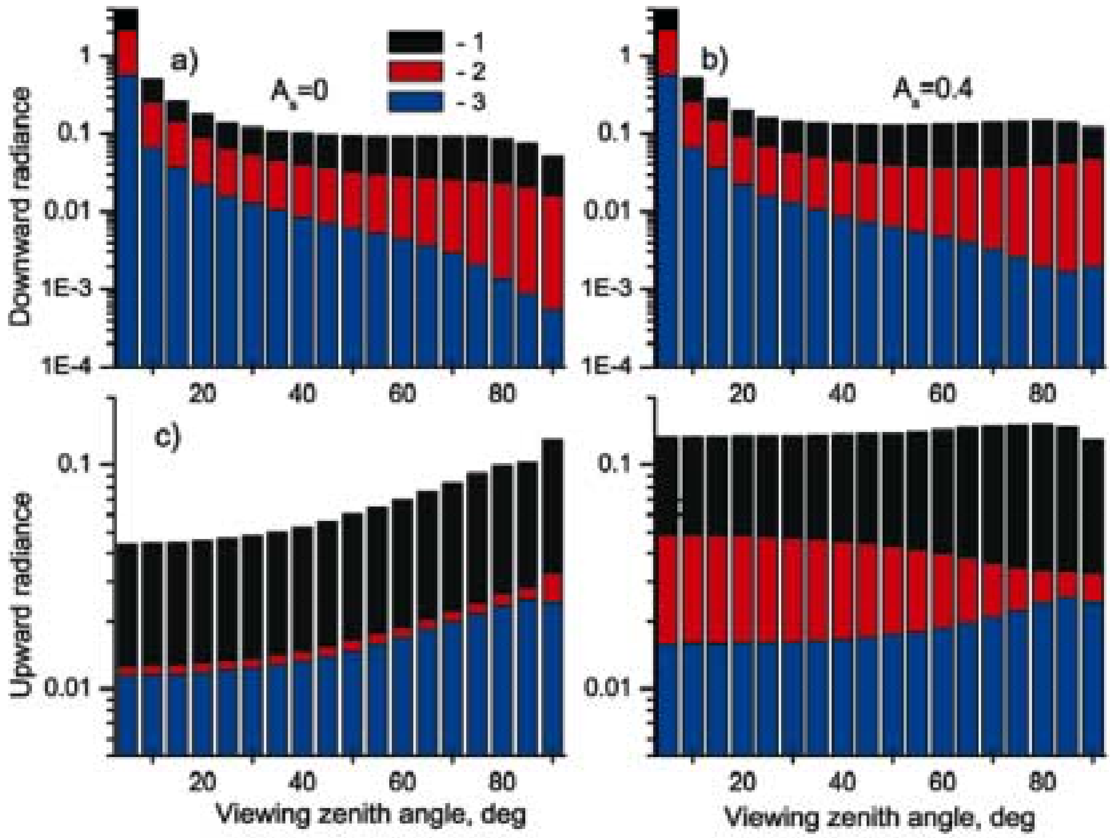

Figure 2. Angular distributions of transmitted (a, b) solar radiance at the bottom boundary and reflected (c, d) radiance at the top boundary of overcast, horizontally-homogeneous cloud layer with optical depth $\tau = 1$ for solar zenith angle $\xi_\oplus = 0$ and different surface albedos: (a, c) $A_s = 0$ and (b, d) A_s - 0.4. Calculations are made for $\lambda = 3.08\mu m$ assuming: no water vapor and ice particle absorption (curve 1), ice particle absorption only (curve 2), and water vapor plus ice particle absorption (curve 3).

If surface albedo $A_s = 0$ and clouds are optically thin, then the qualitative character of $\tilde{I}^{\uparrow(\downarrow)}$ variations with observation angle will be determined by the shape of the scattering phase function (Figure 1). The presence of absorption in the medium leads to quantitative changes. As expected, the downward radiance is reduced considerably, while changes in upward radiance are significant, once water vapor absorption is considered in addition to the absorption by ice particles (Figures 2a, 2c, and Histograms 2 and 3).

Switching to $A_s > 0$ case, in the absence of water vapor absorption the surface-reflected radiation contributes considerably to upward radiance. This contribution is most significant for viewing directions close to zenith, the reason why $\tilde{I}^{\uparrow}(A_s > 0)$ differs qualitatively from $\tilde{I}^{\uparrow}(A_s = 0)$. The water vapor absorption decreases the fraction of radiation reaching the surface, so the latter influences $\tilde{I}^{\uparrow}(A_s > 0)$ weaker, the reason why $\tilde{I}^{\uparrow}(A_s > 0)$ and $\tilde{I}^{\uparrow}(A_s = 0)$ differ much less in this case (Figures 2c, 2d, and Histogram 3).

To estimate the influence of stochastic cloud geometry on $\tilde{I}^{\uparrow(\downarrow)}$ in presence of ice particle and H_2O absorption, compare calculations made for horizontally homogeneous cloud model (PP-cloud) with those for broken ice-crystal clouds (3D-clouds). We consider a cloud field consisting of cloud bands with characteristic extents D_x and D_y and along OX- and OY-axes, respectively. The bandwidth D_x is assumed to be comparable with cloud geometrical thickness H and much less than the band length D_y. Such a spatial pattern is characteristic of the cirrus clouds and is frequently observed for Ci clouds.

For optically thin clouds (Figure 3) the angular distributions of transmitted and reflected radiation qualitatively agree but, since 3D clouds have more scattered radiation, we get $\tilde{I}^{\uparrow(\downarrow)}(3D) \geq \tilde{I}^{\uparrow(\downarrow)}(PP)$. For instance, for viewing angles close to solar zenith, the neglect of stochastic cloud field structure may

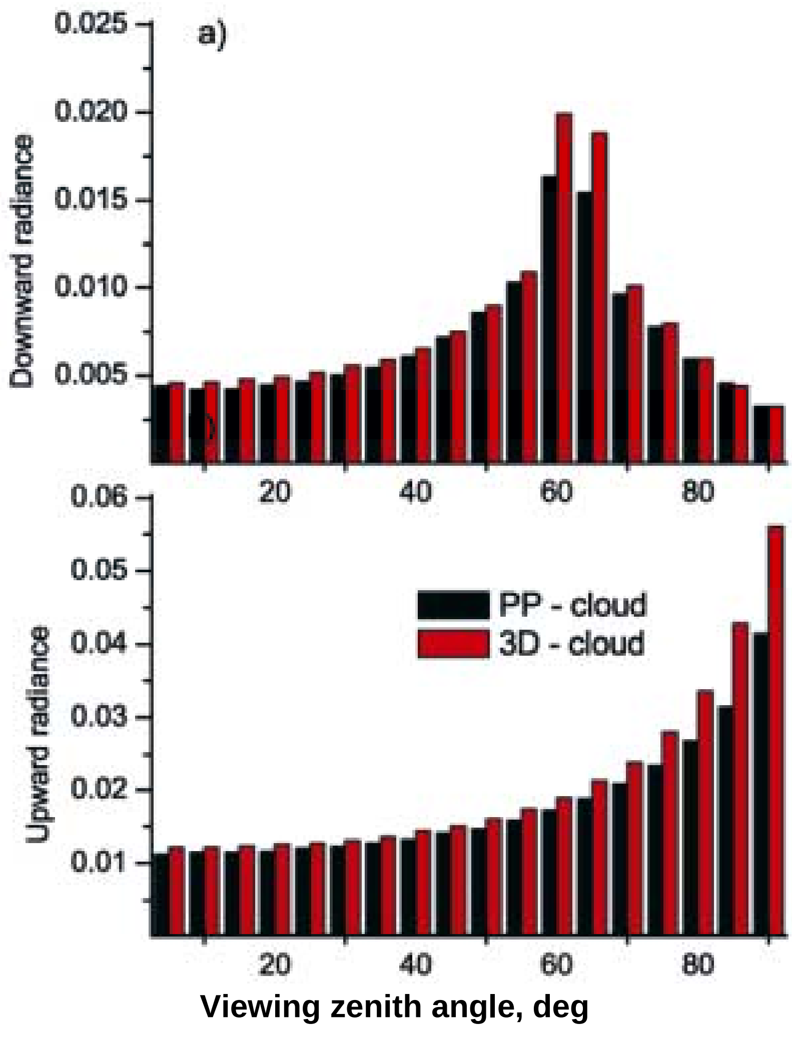

Figure 3. Angular distributions of solar radiation calculated with (3D-cloud) and without (PP-cloud) account of random cloud geometry for wavelength $\lambda = 3.08\mu m$; optical depth $\tau = 1$; solar zenith angle $\xi_{\oplus} = 60°$; cloud fraction N = 0.5; and surface albedo $A_s = 0.2$.

lead to underestimation of $\tilde{I}^{\downarrow}$ by 20% to 25%. As optical thickness of clouds increases, the changes in the angular structure of radiation become more significant, leading to violation of inequality above for certain viewing angles.

Figure 4 shows angular distributions of solar radiation calculated in 3D cloud model for different wavelengths. The $\tilde{I}^{\uparrow(\downarrow)}$ variations caused by the scattering properties of optically thin ice clouds are much more significant than those due to effects of random cloud field geometry, consistent with our earlier findings for visible wavelengths (λ = 0.63μm) (Petrushin and Zhuravleva, 2000).

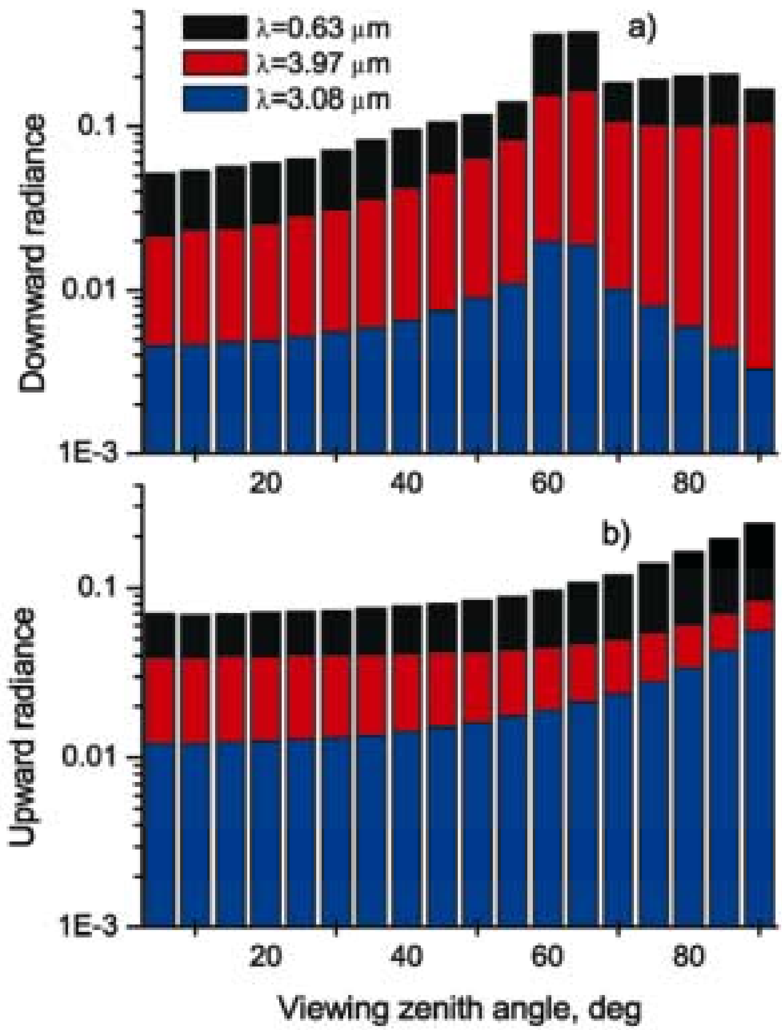

Figure 4. Angular distributions of solar radiation for different wavelengths in 3D cloud model. Calculations are made for optical depth τ = 1; solar zenith angle $\xi_{\oplus}$ = 60°; cloud fraction N = 0.5; D_x = 2 km, D_y = 100 km; and surface albedo A_s = 0.2.

Acknowledgment

The work is supported partially by the Russian Fund for Basic Research (through the Grant 00-05-65456).

References

Cai Q., and K. N. Liou, 1985: Calculation on the light scattering function of hexagonal ice crystals. *Adv. Atmos. Sci*., **2**, N 4 , 446 - 454.

Fu, Q., B. Carlin, and U. Lohmann, et al., 2000: Cirrus horizontal inhomogeneity and solar albedo biases. In *IRS-2000*: Current problems in atmospheric radiation, Abstract, p. 63.

Fu, Q., and K. N. Liou, 1993: Parameterization of the radiative properties of cirrus clouds. *J. Atmos. Sci*., **50**, 2008-2025.

Heymsfield A. J., and G. M. R. Platt, 1984: A parameterization of the particle size spectrum of ice clouds in terms of the ambient temperature and the ice water content. *J. Atmos .Sci*., **41**, 846-855.

Liou, K. N., and N. Rao, 1996: Radiative transfer in cirrus clouds, IV: On cloud geometry, inhomogeneity, and absorption. *J. Atmos. Sci*., **53**, 3046-3065.

Macke A., R. Scheirrer, and L. V. Bremen, 2000: A statistically based parameterization of shortwave cloud radiative fluxes for inhomogeneous mixed phase clouds. In *IRS-2000*: Current problems in atmospheric radiation, Abstract, 64-65.

Mitchell, D. L., A. Macke, and Y. Liu, 1996: Modeling cirrus clouds. Part II: Treatment of radiative properties. *J. Atmos. Sci*., **53**, 2967-2988.

Moskalenko, N. I., 1969: Spectral transmission functions in the band of H_2O vapor and O3, N2O, N2 constituents in the atmosphere. *Izv. Acad. Sci USSR Atmos. Oceanic Phys*, **11**, 1179-1190.

Petrushin A. G., 1998: Optical radiation scattering and absorption in a crystalline cloud medium. Problems of Clouds Physics, ed. L. P. Semenov, St. Peterburg, Gidrometeoizdat, 118-149. (In Russian).

Petrushin A. G., and T. B. Zhuravleva, 2000: Influence of ice particle shape on albedo and transmittance of ice-crystal clouds. In *Proceedings of the Tenth Atmospheric Radiation Measurement (ARM) Science Team Meeting*, U.S. Department of Energy, Washington, D.C. Available URL: http://www.arm.gov/docs/documents/technical/conf_0003/petrushin-ag.pdf

Sundqvist H., 1993: Inclusion of ice phase of hydrometeors in cloud parameterization for mesoscale and largescale models. *Beitr. Phys. Atm*., N 66 , 445-453.

Titov, G. A., T. B. Zhuravleva, and V. E. Zuev, 1997: Mean radiation fluxes in the near-IR spectral range: Algorithms for calculation. *JGR*, **102**, 1819-1832.

Warren, S. G., 1984: Optical constants of ice from ultraviolet to the microwave. *Appl. Opt*., **23**, 8, 1206-1225.